Adaptation of bacterial proteome reveals a key role of the cell envelope in starvation survival

Severin Schink[1, *, #], Constantin Ammar[1,2,*], Yu-Fang Chang[1],
Ralf Zimmer[2] and Markus Basan[1, #]

[1] Systems Biology Department, Harvard Medical School, 200 Longwood Ave, 02115 MA, USA
[2] Institute of Informatics, Ludwig-Maximilians-Universität München, Amalienstr. 17, 80333, Munich, Germany
* Contributed equally
[#] Correspondence: severin_schink@hms.harvard.edu and markus@hms.harvard.edu

Abstract

Bacteria reorganize their physiology and proteome upon entry to stationary phase. What part of this reorganization improves starvation survival is a difficult question, because the change in physiology includes a global reorganization of the proteome, envelope and metabolism of the cell. In this work, we aim to disentangle causation from correlation and identify changes in proteome resource allocation and physiology that directly contribute starvation survival. We found that a fundamental trade-off between fast growth and long survival is set by proteome allocation across diverse growth conditions and utilize this trade-off to statistically score over 2000 *E. coli* proteins for their global correlation with lifespan. The combined ranking allowed us to narrow down the set proteins that positively correlate with survival and validate the causal role of these proteins in improving starvation survival. Remarkably, we found that a significant fraction of survival genes is related in the cell envelope, i.e., periplasm and outer membrane. Indeed, we confirmed that the envelope integrity of *E. coli* plays a crucial role during starvation and verified that improving the mechanical stability of the outer membrane leads to better survival. Our results uncover a new protective feature of the outer membrane that adds to the growing evidence that the outer membrane is not only a barrier that prevents abiotic substances from reaching the cytoplasm, but essential for bacterial proliferation and survival.

Introduction

Nutrient limitation is a defining part of the lifecycle of microorganisms. In the absence of external nutrients, the only energy sources for heterotrophic organisms is either internal storage (Fung and Kwong, 2013; Hengge-Aronis and Fischer, 1992; Strange, 1968) or nutrients retrieved by recycling dead biomass (Finkel, 2006; Schink et al., 2019; Zambrano and Kolter, 1996). This finite energy source can be temporarily used to maintain the cell, but will eventually deplete, exposing cells to a slow deterioration process driven by entropic forces. It was previously shown that the survival kinetics during starvation, i.e. how many cells will be still alive after a certain time, is determined by the consumption rate of these nutrients, called the maintenance rate, and the availability of nutrients (Schink et al., 2019). Because maintenance rate is a major determinant of bacterial lifespan, we expect bacteria to minimize their maintenance cost to maximize fitness in starvation. But what determines how much maintenance bacteria need to perform, and how they can reduce it is still largely unclear.

The question of maintenance is particularly puzzling, because sporulating organisms can minimize the number of active processes - without losing their viability. The maintenance rate of non-sporulating bacteria is similarly not an engraved biophysical constant. Instead, *Escherichia coli*, for example, can decrease its maintenance rate and death rate over 5-fold in response to environmental cues sensed during the prior growth phase (Biselli et al., 2020).

But identifying the part of the adaptation that determines lifespan is tricky as the bacteria globally reorganize their proteome (Hui et al., 2015; Schmidt et al., 2016), macromolecular composition (Bremer and Dennis, 2008; Schaechter et al., 1958) and even morphology (Schaechter et al., 1958), when nutrients get depleted and growth slows down. This means that most properties of bacteria correlate or anti-correlate with lifespan. In addition, while several regulators and genes have been identified that react to nutrient depletion and are essential for survival, such as the general stress response regulator *rpoS* (Hengge-Aronis and Fischer, 1992), cAMP-Crp (Makman and Sutherland, 1965; Notley-McRobb et al., 1997), stringent response (Magnusson et al., 2003; Irving et al., 2021) or DNA protection in starvation *dps* (Almirón et al., 1992), there is no evidence that these systems are the limiting factors for survival.

In this paper, we analyzed diverse growth conditions and find that they heavily influence lifespan after nutrients run out. Due to the diversity in proteomic responses, we can use this information to narrow down the set of proteins that correlate with better survival and identify which parts of the adaptation causally determine lifespan of *E. coli* in starvation.

Results

Proteome analysis identifies proteins and processes that correlate with long lifespan

We studied *Escherichia coli* K-12, first grown in single carbon source N^+C^+ minimal medium, followed by a wash and resuspension in medium with the carbon source missing. During the ensuing starvation, viability decreases exponentially (Phaiboun et al., 2015; Schink et al., 2019), with death rate depending on the previous growth condition. *E. coli* grown on carbon substrates supporting faster growth die faster than those on poor carbon substrates (Biselli et al., 2020). We suspected that changes in the proteome composition, which is known to vary highly across growth conditions (Hui et al., 2015; Schmidt et al., 2016), are at least partially responsible for the observed changes in death rate. However, in a single growth perturbation, such as varying the carbon substrates, over half of all proteins were up- or downregulated (Hui et al., 2015; Schmidt et al., 2016), making it impossible to pinpoint individual proteins or processes as being responsible.

To narrow down the search for the proteins that determine lifespan, we decided to use additional growth conditions that show different changes in proteome. We identified a total of six independent perturbations, which we collectively call ‘CARLOS conditions’ that affect proteome composition and death rate. Among these, those that reflect a change in nutrient availability (C:

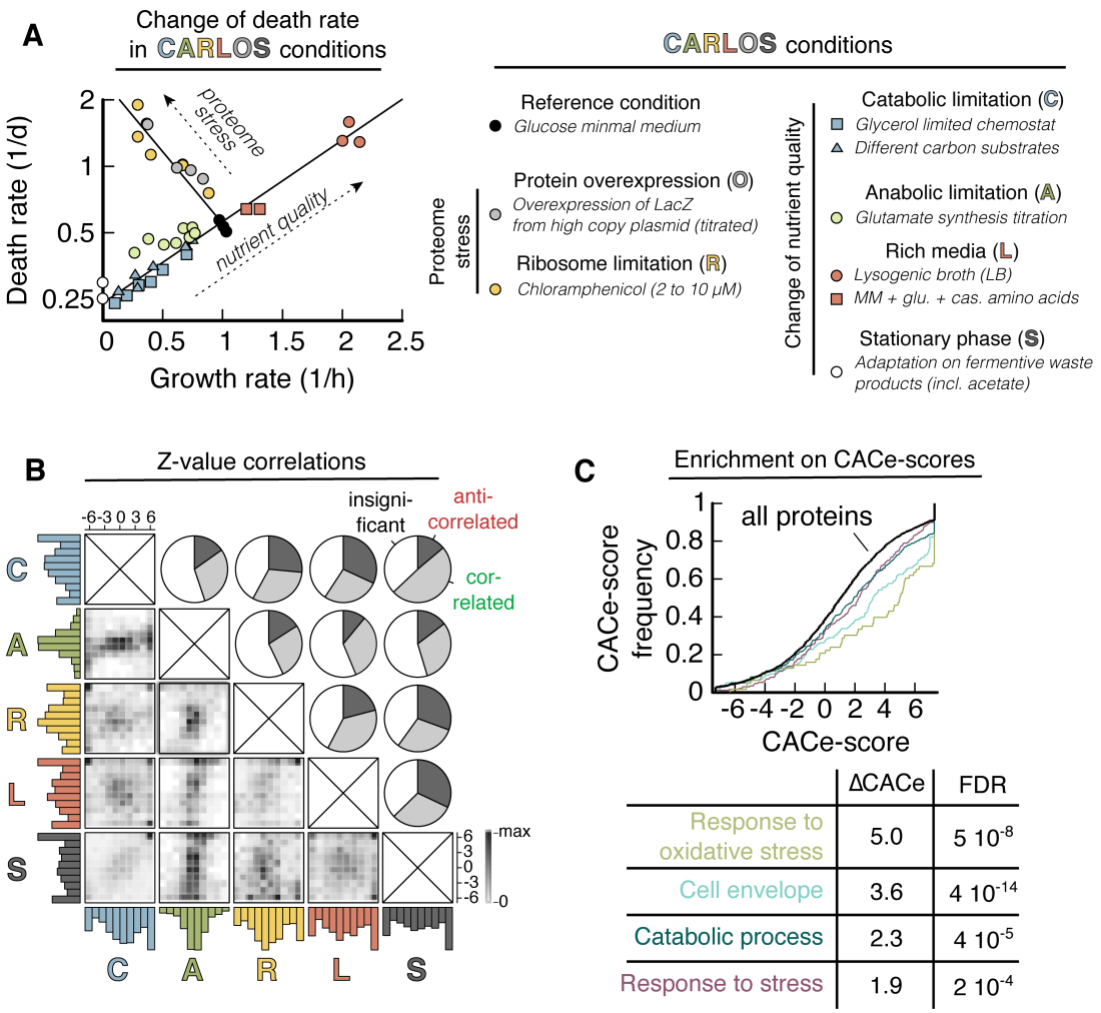

Figure 1 Proteome composition and death rates in CARLOS conditions. (**A**) Death rate versus pre-starvation growth rate on a semilog-plot. CARLOS conditions are defined in legend. CARLOS conditions that perturb nutrient quality (C, A, L and S) lead to an exponential increase of death rate. Conditions that stress the proteome (R and O) show an orthogonal exponential increase with slower growth. Each data point is a single experiment. Chemostat (C) and parts of (L) are from Ref. (Biselli et al., 2020). See Table S1 for data. (**B**) Pair-wise comparison of protein Z-values between all CARLOS conditions. Z-values measure the correlation between abundance and death rate in a single condition for a single protein, see Methods. Z-values calculated from different data sets of similar perturbations are highly correlated (Fig. S3A&B) and are used to create composite Z-value for each protein (Fig. S3C), which are shown in the colored histograms of this panel. (**C**) Z-values are merged into a single 'Combination of Additive Certainties' score (abbr. 'CACe-score') for each protein that measures correlation of abundance with survival across all experiments, see Fig. S2 and Methods. Several GO-processes are significantly enriched towards higher scores, i.e., positive correlation, compared to the background of all proteins (black).

catabolic limitation, A: anabolic limitation, L: rich media (LB) and S: stationary phase) collapse

onto a single exponential increase of death rate with growth rate, while conditions that perturb the proteome by expression of excess proteins (R: ribosome limitation, O: LacZ overexpression) fall onto an orthogonal exponential increase (Fig. 1A).

CARLOS conditions result in substantial changes in proteome composition. We analyzed these changes in the proteome using published proteomics data from three different repositories (Houser et al., 2015; Hui et al., 2015; Schmidt et al., 2016), which individually cover a subset of the CARLOS conditions (C, L & S in Ref. (Schmidt et al., 2016), C, A & R in Ref. (Hui et al., 2015) and S in Ref. (Houser et al., 2015)). To be able to compare proteins across conditions and across data sets, we created a composite statistical score to measure the probability that the abundance of a protein is significantly correlated or anticorrelated with longer survival (Fig. S1 for a graphical summary and Methods for details). Regulation between datasets is compared in a pairwise fashion and regulation is expressed as Z-values. Z-values of individual data sets of similar conditions are integrated (Fig. S2), to derive a Z-value for each condition (Fig. 1B, colored histograms show Z-value distributions). Here we had to exclude 'O, LacZ overexpression' due to lack of sufficient statistical data, shortening CARLOS to CARLS, but we will integrate qualitative information from this condition below.

By comparing Z-values of the conditions in a pair-wise manner, we confirmed that proteome changes in the remaining CARLS conditions are partially independent of each other, as evidenced by a significant fraction of Z-values being anti-correlated in each comparison, which can help us narrow down the target set of proteins (Fig. 1B, heat maps and pie charts). We integrated Z-values of the individual CARLS conditions into a single 'Combination of Additive Certainties' score (abbrv. 'CACe score'), that measures the global correlation strength of proteins with lifespan (Fig. S1 and Methods). The resulting list of Z-values and CACe scores for over 2000 proteins is available in Table S2.

Fractions of the proteome determining death rate can be either beneficial or harmful. To understand which of these fractions is dominant, we used the 'O' condition, where overexpression of a useless protein leads to a decrease in the abundance of virtually all proteins simultaneously (Fig. S3). This condition led to a 5-fold increase in death rate (Fig. 1A, gray symbols), as we would expect for

largely beneficial proteins determining death rate. Thus, we restricted our further analysis to positive CACe-scores, where a higher abundance correlates with longer lifespan across conditions.

Finally, we used CACe-scores to identify GO-processes and cellular compartments that contain proteins with significantly larger CACe-scores than average. Using a Kolmogorov-Smirnov test, we evaluated enrichment of proteins in GO-processes and compartments (Table S3) and identified 'oxidative stress response', 'response to stress', 'catabolic process' and 'cell envelope' as highest scoring GO-processes (Fig. 1C). We next wanted test if any of these processes/compartments causally affect bacterial lifespan.

Death rate depends on the integrity of the cell envelope

The response to oxidative stress had the highest CACe score in our analysis, with proteins such as catalases KatE (CACe-score: 7.3) and KatG (7.3), superoxide dismutase sodA (5.1), and hydroperoxidase AhpC (5.7), all of which are essential to *E. coli's* adaptation to stress (Farr et al., 1988; Farr and Kogoma, 1991; Dukan and Nyström, 1999; Chiang and Schellhorn, 2012), correlating well with survival across CARLOS conditions. Therefore, we first tested whether oxidative stress limits lifespan of starving bacteria by starving bacteria in anaerobic conditions, where the rate oxidative damage should be absent. It was previously reported that starved *E. coli* suffer from protein carbonylation and that anaerobic conditions can prevent carbonylation and stop death (Dukan and Nyström, 1999). However, to our surprise, our results showed the opposite. We found that death rates in anaerobic conditions were even faster than in aerobic conditions (Fig. S4A). This did not depend on whether growth prior to starvation was in aerobic or anaerobic conditions. Similarly, adding antioxidants that prevent carbonylation (glutathione, ascorbic acid or mercaptoethanol) did not decrease death rate (Fig. S4B).

Also, we could not confirm the causal role of the general 'response to stress', despite its high score. Neither inducing its expression using heat shocks, low pH nor high osmolarity during growth, all of which significantly increase abundance of 'response to stress' proteins (Fig. S5A-C), resulted in changes of death rate (Fig. S5D). This absence of the cross-protection can be reconciled with what is known about the stress response in *E. coli*. While knock-outs of the general stress response regulator *rpoS* show increased death rates (Hengge-Aronis and Fischer, 1992), they do not remove

the growth-death dependence in carbon limitation (Biselli et al., 2020) that forms the basis of our analysis. This suggests that while some stress response genes are essential for optimal starvation survival (likely because rpoS dependent genes help recycling nutrients (Schink et al., 2019)), they are not limiting and not responsible for the modulation of death rates in the CARLOS conditions (Fig. 1A).

Another high-scoring class of proteins identified by our analysis were proteins of the cell envelope, which includes the periplasm, cell wall and outer membrane (Fig. S6 for graphical summary). Proteins associated with the cell envelope make up about 13% of the proteome in rich nutrient conditions, and up to a staggering 23% for bacteria adapted to stationary phase (Fig. 2A and Table S4). In addition to the GO analysis, we also noticed the cell envelope in a knock-out screen of high-scoring, non-essential genes. The fastest dying knock-out, Δ*lpp,* encoded a protein that is located in the cell envelope (Table S5). In contrast, most other genes, especially those belonging to stress response and oxidative damage showed little or no change of death rates (Table S5), further corroborating that they are non-limiting.

The physiological role of Lpp (CACe-score: 6.1), together with OmpA (6.6), is to physically link outer membrane and cell wall. These proteins are essential for the cell envelope's mechanical integrity, and make up around half the cell envelope proteome and up to 12% of the total proteome (Fig. 2A). Motivated by this finding, we tested more cell envelope proteins, and found that starvation-survival is highly sensitive to knock-outs across different functionalities of the cell envelope (Fig. 2B), from outer membrane protein folding (BamE & Skp), cell wall synthesis and modification (Prc, NlpI, DolP & NlpD), phospholipid recycling (MlaA & MlaC) to cell envelope regulators (CpxA & rseA).

Conversely, only knockouts of porins, which facilitate diffusion of biomolecules across the outer membrane, have high CACe-scores, and are highly abundant (Fig. 2A), did not change death rate (Fig. 2B).

This sheer abundance of cell envelope proteome makes it a compelling candidate for determining death rate, as it would mean adaptation to optimal starvation survival would require a major

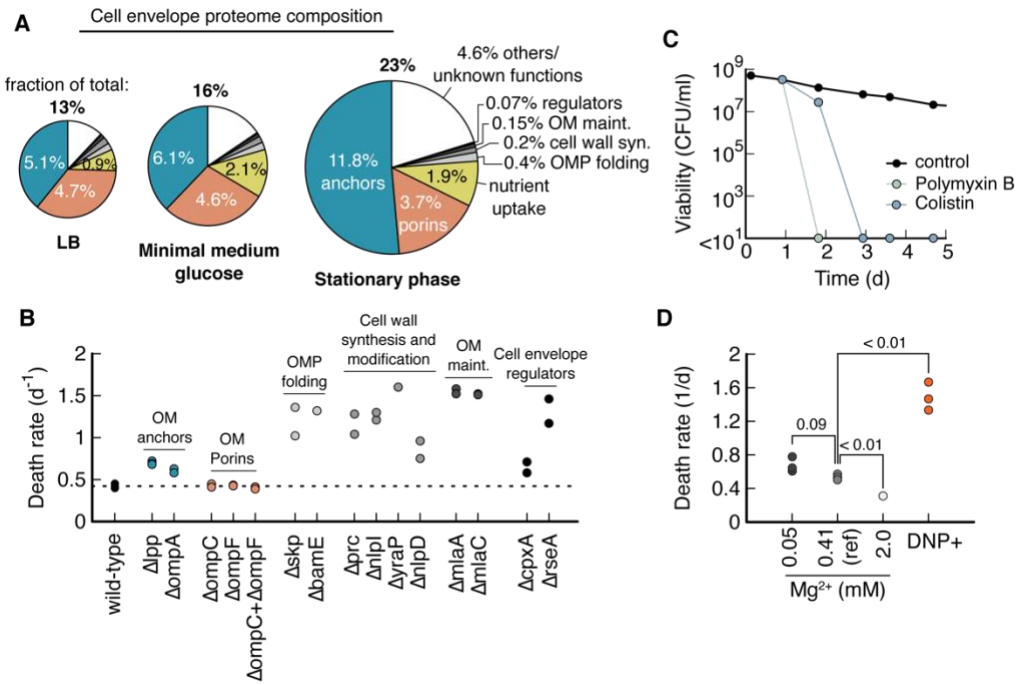

Figure 2 **Cell envelope integrity plays a major role in starvation survival.** (**A**) Proteome composition of the cell envelope (see Fig. S6 for details on the cell envelope structure). Size of pie indicates fraction of total proteome that is associated with envelope. Outer membrane anchors (Lpp and OmpA) constitute half of the cell envelope proteome. Major porins (OmpC and OmpF) and nutrient uptake (large number of binding proteins) constitute other major fractions. Quantification of abundancies are in Table S4 (**B**) Knock-out of several genes with different functionalities in the cell envelope increase death rates. (**C**) Polymyxin B and Colistin, added daily, first dose at 24h. Antibiotic concentration was 10x minimum inhibition concentration during growth (MIC). Each data point is the average of three biological repeats. Viabilities indicated at $<10^1$ mean no colonies were detected from 100 µl culture. (**D**) Death rates for different Mg^{2+} concentrations. Reference condition (black circle in Fig. 1A) is at 0.41 mM Mg^{2+}. DNP+ cultures were supplemented with 1 mM 2,4-dinitrophenol during starvation in reference medium. Each data point is from a single experiment. P-values (Student's t-test) are indicated in comparison to the reference condition.

reorganization of the proteome, rather than simply synthesizing a small set of proteins that could be achieved with a limited amount of stored nutrients. This could explain why the prior growth condition has such a big influence on starvation survival.

Many of the knock-outs that we identified are known to impair the mechanical integrity of the cell envelope (Bryant et al., 2020; Malinverni and Silhavy, 2009; McBroom et al., 2006; Rojas et al., 2018; Schäfer et al., 1999; Suzuki et al., 1978; Tsang et al., 2017; Yem and Wu, 1978). Therefore,

we hypothesized that the mechanical integrity of the cell envelope is plays a causal role in survival. To test this hypothesis, we applied antibiotics that are known to compromise the cell envelope, polymyxin B and colistin. Both antibiotics were highly effective when added 24 h into starvation, killing the entire population within 24 h and 48h, respectively (Fig. 2C). This is unusual, as most other antibiotics are ineffective on starving bacteria (Schink et al., 2021). Polymyxin B and colistin insert into the outer membrane between lipid A molecules and displace Mg^{2+} ions that shield repulsive negative charges between lipid A (Moore et al., 1986). Similarly, supplementing the starved culture with EDTA, a chelator of Mg^{2+} ions that increases permeability (Vaara, 1992), increased death rate 2.8-fold (Fig. 2D).

These results show that cell envelope integrity is essential for survival. In addition, we wanted to know if cell envelope integrity is also limiting survival, and tested the reverse effect by increasing Mg^{2+} concentrations. Indeed, we found a 40% drop in death rate at high Mg^{2+} concentrations compared to the reference condition (Fig. 2D), confirming that cell envelope integrity is both essential and limiting.

Ion homeostasis and cell envelope integrity account for the variation of starvation survival

But how does cell envelope integrity influence survival? We recently showed that the cost of ion homeostasis is a major determinant of lifespan of bacteria in carbon starvation. Based on this work, we hypothesize that changes in death rates in the CARLOS conditions were due to changes in the cost of ion homeostasis, mediated by the envelope proteome affecting membrane permeability. If membranes are less permeable, less energy is required to actively pump ions across the cytoplasmic membrane to remain ion homeostasis. This reduction in maintenance should then result in a lower death rate (Schink et al., 2019).

To test this hypothesis we used an osmo-balanced medium with low salt concentrations, designed to minimize the content of inorganic ions that can diffuse across membranes (Schink et al., 2021). This medium reduces the death around 5-fold in standard glucose minimal medium conditions (Schink et al., 2021). If changes in the membrane permeability are responsible, we predict that the osmo-balanced medium should not just reduces death rates, but also removes the growth-death dependence that we found in Fig. 1A. Indeed, the osmo-balanced medium abolished the

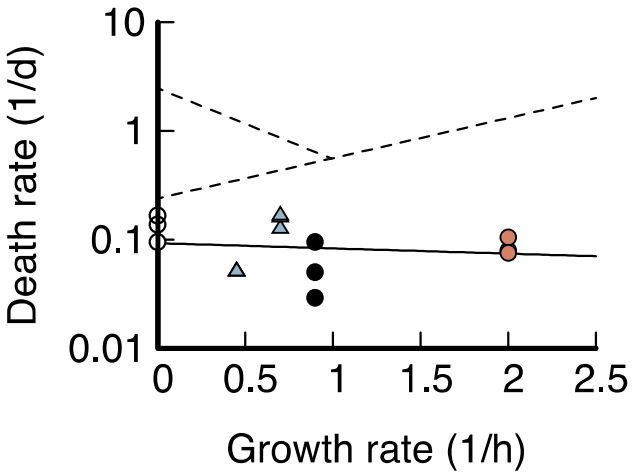

Figure 3 **Death rates in osmo-balanced medium.** Death rate plotted versus growth rate on a semi-log scale for experiments in 'osmo-balanced' medium. Colors indicate stationary phase (S - 'white'), carbon limitation (C - 'blue'), reference ('black') and rich medium (L - 'red'), as defined in Fig. 1A. The data and shows no correlation with growth rate; solid black line is an exponential fit to the data ($R^2 = 0.02$). Dashed lines are the exponential fits to the CARLOS data in Fig. 1A.

characteristic growth rate dependence of the CARLOS condition (Fig. 3). This confirms that differences of the cell envelope integrity and membrane permeability underlie the variations in death rate seen in Fig. 1A.

Discussion

We performed an analysis of proteomics data to identify proteins, processes and cellular compartments that contribute to improved survival of carbon starvation. We identified cell envelope proteome and the membrane permeability as key determinants of survival.

Cost of building a strong cell envelope

Building a strong cell envelope is a costly endeavor. A third of the dry weight of a typical cell consists of cell envelope biomass, half of which consists of protein, and the other half phospholipids, LPS and cell wall (Neidhardt, 1996). Given the substantial fraction of biomass devoted to the cell envelope, it is reasonable that bacteria reduce this biomass investment into the

cell envelope in favorable growth conditions, and instead focus on maximizing their growth rate. However, because of the magnitude of the biomass investment into the cell envelope, bacteria cannot easily adapt to starvation using carbon stores after sudden nutrient depletion, which would explain why pre-growth conditions have such a big effect on starvation survival, and why optimal survival requires prolonged adaptation.

Role of the outer membrane in cell envelope integrity and starvation survival

Surprisingly, many of the proteins that we found to affect survival rates in carbon starvation are related to the outer membrane and overall, our data demonstrates an important role of the outer membrane for starvation survival. While the outer membrane is known to be a permeability layer, in particular to antibiotics, it is less clear how it could achieve a similar effect for inorganic ions, which would explain improved survival in starvation. Ion export pumps, such as NhaA, are thought to only span the cytoplasmic membrane, meaning that ion gradients across the outer membrane should equilibrate. In this case, the outer membrane should offer little protection from inorganic ions. Indeed, in 'plasmolysis' from osmotic shocks, the inner membrane contracts as a result of osmotic pressure, while the outer membrane largely maintains its shape (Rojas et al., 2018), indicating that osmolytes readily diffuse into the periplasm. There is, however, considerable biochemical and mechanical interplay between inner and outer membrane that could contribute to permeability changes. Both membranes share phospholipids, and the outer membrane is involved in recycling lipids that have accumulated on the outer leaflet of the outer membrane (Malinverni and Silhavy, 2009). Recently, the outer membrane has been found to mechanically stabilizes the inner membrane, e.g., via the tol-pal system, which is essential for bacteria to reach plasmolysis in starvation (Rojas et al., 2018; Shi et al., 2021). Integrity of the cell envelope could also protect periplasmic proteins from damage. We therefore argue that a mechanically strong cell envelope allows Gram-negative bacteria to stabilize and protect its cytoplasmic membrane, allowing bacteria to reduce their maintenance cost and increase their lifespan.

Author contribution

SJS, CA and MB conceived the project. SJS and CA performed experiments and proteomics analysis. YFC constructed strains. RZ supervised proteomics analysis. SJS, CA, RZ and MB wrote the paper.

Methods

Strains

All strains used in this study are derived from wild type *E. coli* K-12 strain NCM3722 (Soupene et al., 2003). Strains NQ381 (attB:Plac-xylR, Km-Pu-lacY) was used for 'catabolic limitation' and was described in Ref. (You et al., 2013). In NQ381 strain the expression of the lactose transporter lacY is induced using 3-Methoxybenzamide (3MBA). NQ393 (ΔgdhA+plac-gltBD, attB(phage):lacIQ-tetR::Sp, ΔlacY) was used for 'anabolic limitation' and is described in Ref. (Hui et al., 2015). Using isopropylthio-β-galactoside (IPTG), the expression of gltBD is induced, which encodes glutamate synthase. NQ1389 (Ptet-tetR on pZA31; Ptetstab-lacZ on pZE1) was used to overexpress LacZ using chlortetracycline (cTc) as inducer and is reported in Ref. (Basan et al., 2015a). All knockouts shown in Fig. 2 were transferred from the Keio collection (Baba et al., 2006) to NCM3722 via P1 transduction to yield strain. Knockouts from Table S5 are taken from the Keio collection and transferred to NCM3722.

Culture medium

The culture medium "N^-C^- minimal medium" (Csonka et al., 1994), contains 1g K2SO4, 17.7 g K2HPO4, 4.7 g KH2PO4, 0.1 g MgSO4·7H2O and 2.5 g NaCl per liter. The medium was supplemented with 20 mM NH4Cl, as nitrogen source, and varying carbon sources. The 'reference glucose condition' contained 0.2% glucose. All chemicals were purchased from Sigma Aldrich, St. Louis, Mo, USA. The 'osmo-balanced' medium is described in (Schink et al., 2019), and contains 0.2 M MOPS (3-(N-morpholino)propanesulfonic acid), titrated to pH 7 with KOH, and 1 mM $MgCl_2$, 0.1 mM $CaCl_2$, 0.16 mM K_2SO_4, 0.5 mM K_2HPO_4, 22mM NH_4Cl and lacks a carbon source. Cultures starved in the 'osmo-balanced' medium were previously grown in N-C- medium supplemented with NH_4Cl and glucose.

Culture conditions

Prior to each experiment, bacteria were streaked out from -80ºC glycerol stock on an LB agar plate supplemented with antibiotics if necessary. Bacteria were cultured in three steps. First, a seed culture was grown in lysogenic broth (LB) from a single colony. Second, the seed culture was diluted in N^-C^- minimal medium supplemented with 20 mM NH_4Cl and a carbon source and

grown overnight for at least 5 doublings to exponential phase. The next morning, the overnight culture was diluted into fresh, pre-warmed $N^{-}C^{-}$ minimal medium supplemented with 20 mM NH_4Cl and a carbon source and grown for another 5 to 10 doublings. At an optical density of 0.5 or below, the culture was washed by centrifugation (3 min at 3000 g) and resuspension into fresh, carbon-free, pre-warmed $N^{-}C^{-}$ minimal medium supplemented with 20 mM NH_4Cl. This washing step removes excreted byproducts such as Acetate. For growth conditions known to fully respire carbon, e.g. wild-type NCM3722 grown on glycerol (Basan et al., 2015b), this washing step was omitted.

NQ381 was grown overnight and during the experimental culture with the inducer concentrations indicated in Table S1. NQ1389 was grown without inducer overnight, with indicated inducers added after dilution of the overnight culture, to prevent escape mutations and plasmid loss. NQ399 was grown with 100 µM IPTG overnight and the indicated IPTG concentrations after dilution of the overnight culture.

For small culture volumes (5 to 7 ml), 20 mm x 150 mm glass test tubes (Fisher Scientific, Hampton, NH, USA) with disposable, polypropylene Kim-Kap closures (Kimble Chase, Vineland, NJ, USA) were used.

Viability measurements

For viability measurements, cultures were diluted in untreated, sterile 96 well plates (Celltreat, Pepperell, MA, USA) in three to four steps using a multichannel pipette (Sartorius, Göttingen, Germany) to a target cell density of about 4000 CFU/ml. 100 µl of the diluted culture was spread on LB agar plates supplemented with 25 µg/ml of 2,3,5-triphenyltetrazolium chloride to stain colonies bright red using Rattler Plating Beads (Zymo Research, Irvine, CA, USA), and incubated for 12 to 24 hours. Images of agar plates were taken with a Canon EOS Rebel T3i (Tokyo, Japan) mounted over an LED light box ‘Lightpad A920’ (Artograph, Delano, MN, USA), and analyzed using a custom script in Cell Profiler (Carpenter et al., 2006). Colony forming units per volume (CFU/ml) were calculated by multiplying the number of colonies per agar plate by the dilution factor.

Stress conditioning

For pre-stressing, wild-type *E. coli* NCM3722 was grown in glucose minimal medium, either in a water bath at 40ºC ('heat stress'), in medium supplemented with 50 mM NaCl ('osmotic stress') or in $N^{-}C^{-}$ medium adjusted to pH 6 using KOH ('pH stress'). At an optical density $OD6_{00}$ of about 0.5, cultures were washed and transferred to pre-warmed, carbon-free $N^{-}C^{-}$ supplemented with 20 mM NH_4Cl, and the decay of viability was recorded for about 10 days.

Anaerobic culturing

For anaerobic growth and starvation, cultures were grown in 0.05% glucose minimal medium in a vinyl anaerobic chamber (COY Lab Products, Grass Lake, Mi, USA), in Erlenmeyer flasks (Chemglass, Vineland, NJ, USA) on a magnetic stirrer (IKA RO10, Staufen, Germany), and not washed after the end of growth. For aerobic growth and anaerobic starvation, cultures were grown in 0.05% glucose minimal medium in an air incubator. At an optical density of about 0.5, cultures were centrifuged, supernatants were discarded, and pellets were introduced to the anaerobic chamber. In the anaerobic chamber, pellets were resuspended in pre-warmed, carbon-free minimal medium. All media were degassed prior to being introduced to the anaerobic chamber, and left with open lid to be equilibrated for one week.

Proteomics data processing

The MS proteomics data was downloaded from the corresponding PRIDE partner repositories (Schmidt et al.: PXD000498, Hui et al.: PXD001467, Houser et al.: PXD002140). For the Schmidt and Houser datasets, the .raw files were downloaded, for the Hui dataset, peptide-intensity mappings were downloaded. The Schmidt and Hui datasets were searched MaxQuant (Cox and Mann, 2008) v. 1.5.7.4 using standard settings and "Label Free Quantification" (LFQ) and "Match between runs". The Schmidt and the Houser datasets were searched against the reviewed Uniprot *E. coli* database (03/2019).

Differential expression analysis of proteomics data

All datasets were processed with the MS-EmpiRe (Ammar et al., 2019) algorithm for differential quantification, which assigned fold changes and significance scores to each protein in a condition pair. For the Schmidt and Houser datasets, the MaxQuant "peptides.txt" and "proteinGroups.txt"

files were used as input. The Hui dataset was pre-processed as follows: As in the experimental setup of Hui et al. the data was quantified relative to a ^{15}N-labelled spike-in, a direct assessment of LFQ values was not optimal. Similar to the approach of Ref. (Geiger et al., 2010), we first assessed the fold changes of each peptide relative to its heavy labeled spike-in. To preserve the intensity information, we re-scaled each spike-in fold change by the median intensity of the spike-in peptide over all conditions. This resulted in pseudo-intensities, which we further processed in a "LFQ-like" manner using MS-EmpiRe.

Z-value based ranking of the proteome perturbations

As displayed in Fig. 2 and discussed in the main text, each growth condition has a corresponding death rate. Additionally, when we compare two conditions with one condition having a lower death rate than the other, we expect the lower death rate to be caused by increased expression of proteins. In our ranking, we hence had to identify proteins that show increased expression for decreased death rate over all conditions.

Our initial dataset consisted of the perturbations "Transporter Titration", "Ribosome Limitation" and "Anabolic Limitation" in the Hui set, "Carbon Substrates", "Chemostat", "Rich Media", "Stationary Phase", "Osmotic Shock", "Heat Stress" and "PH Stress" in the Schmidt set and "Stationary Phase" in the Houser set. Each dataset had a glucose reference condition and the "Stationary Phase", "Osmotic Shock", "Heat Stress" and "PH Stress" perturbations were compared to the corresponding glucose reference using differential expression analysis with MS-EmpiRe. This assigned to each protein a log fold change denoting the change in expression and a significance score denoting the confidence in an expression change.

The remaining perturbations were compared differently. Each condition consisted of several sub-conditions (e.g. different levels of transporter titration in the "Transporter Titration" data set). The sub-conditions were ranked by their corresponding death rate and all combinations were compared in an increasing manner (e.g. C1 vs C2, C2 vs C3, C1 vs C3). This way, positive fold changes always correlate with better survival.

Hence, for each protein G, a multitude of condition pairs CP existed, which had to be combined to a final score. We first applied a Z-value transformation to each CP of protein G as follows:

$$Z_{G,CP} = \mathrm{sgn}\left(FC_{G,CP}\right) \left|\phi^{-1}\left(\frac{p_{G,CP}}{2}\right)\right|, \text{ (eq. 1)}$$

where FC is the log2 fold change, p the p-value determined by MS-Empire, sgn is the signum function and ϕ^{-1} is the inverse standard normal distribution function. The Z-value $Z_{G,CP}$ hence is the distance from zero in a standard normal distribution and can immediately be transformed back into a significance score. The higher the absolute value of the Z-value is, the more significant a measurement is. The Z-value carries both the direction of a regulation (via its sign) and its significance (via its value). Multiple measurements can simply be summed up and the significance of the combined measurements can be assessed via the formula:

$$Z_{\mathrm{G}} = \phi^{-1}\left(\tilde{\phi}\left(\sum_{CP=1}^{n} Z_{G,CP}\right)\right), \text{(eq. 2)}$$

where $\tilde{\phi}$ corresponds to a $N(0,\sqrt{v})$ distribution and v is the variance that depends on the combined random variables.

Generally, the variance of the sum of multiple random variables is the sum over the corresponding covariance matrix. As we only combine variables that follow a standard normal distribution, we can derive the individual covariances in our setup as follows:

When random variables from two independent standard normal distributions are compared, (e.g. Z1 comes from the comparison C1 vs. C2 and Z2 comes from the comparison C3 vs. C4) the covariance is equal to 0. When random variables that share one sample are compared (e.g. Z1 comes from the comparison C1 vs. C2 and Z2 comes from the comparison C1 vs. C3) it can be shown that the covariance is equal to 0.5. This then allows us to determine v and therefore Z_{G}. Z_{G} hence represents the summed $Z_{G,CP}$ but normalized to a standard normal distribution.

Combination of the ranked proteome perturbations

In a first iteration, we applied the procedure described above to all perturbations to assess the overall $N(0,1)$ Z-value of each perturbation (i.e. "Transporter Titration"). This resulted in a list of scored proteins in each perturbation, where a high Z-value means that the protein correlates well with starvation survival. Proteins with scores in less than three perturbations were excluded from the analysis. Depending on the number of samples and the quality of the data, the distributions of the scored perturbations can span different ranges. As we are interested in proteins that score generally well over all perturbations, we re-scaled the individual distributions of scored perturbations with the factor $\mathrm{rs} = \frac{3.09}{Z_{\max}}$, such that the maximum absolute Z-value was 3.09 (corresponds to a p-value of 0.001). Re-scaling was only applied to lower significance (i.e. if $rs < 1$), to prevent that a single perturbation dominated the overall score. The final score was then determined by again assessing normalized $N(0,1)$ Z-Values via equations 1 and 2. Using linear combinations, we ensured, that the overall contributions of CARLS conditions had equal weight. Due to the rescaling before, the final score should not directly be transformed back into an overall p-value, but is a useful measure for an overall ranking. The overall score is robust against missing values, as perturbations that are not available also do not contribute to the variance v of distribution $\tilde{\phi} = N(0, \sqrt{v})$ in equation 2. The available Z-values then contribute more strongly to the overall score.

Absolute quantification of proteins

For absolute quantification, we used protein synthesis rates derived by (Li et al., 2014) from ribosomal sequencing data of a MG1655 glucose reference condition. Synthesis rates were used as proxies for copy numbers and multiplied by the respective molecular weights to obtain mass estimates. Further conditions were compared relatively to the reference with MS-EmpiRe and the mass estimates were scaled by the respective fold changes. To determine the mass fraction of a gene set, the genes of the set were summed and divided by summed mass of all genes.

GO enrichment analyses

The Gene Ontology (GO) was downloaded from http://geneontology.org (03/2019) together with the *E. coli* "ecocyc.gaf" annotation. The relations "is_a" and "part_of" were used for the construction of the gene sets. Score-based analysis was carried out using the Kolmogorov-Smirnov

test with signed scores. Multiple testing correction was carried out via the Benjamini-Hochberg procedure.

References

Almirón, M., Link, A.J., Furlong, D., and Kolter, R. (1992). A novel DNA-binding protein with regulatory and protective roles in starved Escherichia coli. Genes Dev *6*, 2646–2654. https://doi.org/10.1101/gad.6.12b.2646.

Ammar, C., Gruber, M., Csaba, G., and Zimmer, R. (2019). MS-EmpiRe Utilizes Peptide-level Noise Distributions for Ultra-sensitive Detection of Differentially Expressed Proteins. Molecular & Cellular Proteomics *18*, 1880–1892. https://doi.org/10.1074/mcp.RA119.001509.

Baba, T., Ara, T., Hasegawa, M., Takai, Y., Okumura, Y., Baba, M., Datsenko, K.A., Tomita, M., Wanner, B.L., and Mori, H. (2006). Construction of *Escherichia coli* K-12 in-frame, single-gene knockout mutants: the Keio collection. Mol Syst Biol *2*. https://doi.org/10.1038/msb4100050.

Basan, M., Zhu, M., Dai, X., Warren, M., Sévin, D., Wang, Y.-P., and Hwa, T. (2015a). Inflating bacterial cells by increased protein synthesis. Mol Syst Biol *11*. https://doi.org/10.15252/msb.20156178.

Basan, M., Hui, S., Okano, H., Zhang, Z., Shen, Y., Williamson, J.R., and Hwa, T. (2015b). Overflow metabolism in Escherichia coli results from efficient proteome allocation. Nature *528*, 99–104. https://doi.org/10.1038/nature15765.

Biselli, E., Schink, S.J., and Gerland, U. (2020). Slower growth of Escherichia coli leads to longer survival in carbon starvation due to a decrease in the maintenance rate. Molecular Systems Biology *16*, e9478. https://doi.org/10.15252/msb.20209478.

Bremer, H., and Dennis, P.P. (2008). Modulation of Chemical Composition and Other Parameters of the Cell at Different Exponential Growth Rates. EcoSal Plus *3*. https://doi.org/10.1128/ecosal.5.2.3.

Bryant, J.A., Morris, F.C., Knowles, T.J., Maderbocus, R., Heinz, E., Boelter, G., Alodaini, D., Colyer, A., Wotherspoon, P.J., Staunton, K.A., et al. (2020). Structure of dual BON-domain protein DolP identifies phospholipid binding as a new mechanism for protein localisation. Elife *9*, e62614. https://doi.org/10.7554/eLife.62614.

Carpenter, A.E., Jones, T.R., Lamprecht, M.R., Clarke, C., Kang, I.H., Friman, O., Guertin, D.A., Chang, J.H., Lindquist, R.A., Moffat, J., et al. (2006). CellProfiler: image analysis software for identifying and quantifying cell phenotypes. Genome Biol *7*, R100. https://doi.org/10.1186/gb-2006-7-10-r100.

Chiang, S.M., and Schellhorn, H.E. (2012). Regulators of oxidative stress response genes in Escherichia coli and their functional conservation in bacteria. Archives of Biochemistry and Biophysics *525*, 161–169. https://doi.org/10.1016/j.abb.2012.02.007.

Cox, J., and Mann, M. (2008). MaxQuant enables high peptide identification rates, individualized p.p.b.-range mass accuracies and proteome-wide protein quantification. Nat Biotechnol *26*, 1367–1372. https://doi.org/10.1038/nbt.1511.

Csonka, L.N., Ikeda, T.P., Fletcher, S.A., and Kustu, S. (1994). The accumulation of glutamate is necessary for optimal growth of Salmonella typhimurium in media of high osmolality but not induction of the proU operon. Journal of Bacteriology *176*, 6324–6333. https://doi.org/10.1128/jb.176.20.6324-6333.1994.

Dukan, S., and Nyström, T. (1999). Oxidative Stress Defense and Deterioration of Growth-arrested Escherichia coli Cells. J. Biol. Chem. *274*, 26027–26032. https://doi.org/10.1074/jbc.274.37.26027.

Farr, S.B., and Kogoma, T. (1991). Oxidative stress responses in Escherichia coli and Salmonella typhimurium. Microbiological Reviews *55*, 561–585. .

Farr, S.B., Touati, D., and Kogoma, T. (1988). Effects of oxygen stress on membrane functions in Escherichia coli: role of HPI catalase. J Bacteriol *170*, 1837–1842. https://doi.org/10.1128/jb.170.4.1837-1842.1988.

Finkel, S.E. (2006). Long-term survival during stationary phase: evolution and the GASP phenotype. Nat Rev Microbiol *4*, 113–120. https://doi.org/10.1038/nrmicro1340.

Fung, T., and Kwong, N. (2013). Residual Glycogen Metabolism in Escherichia coli is Specific to the Limiting Macronutrient and Varies During Stationary Phase. *17*, 5. .

Geiger, T., Cox, J., Ostasiewicz, P., Wisniewski, J.R., and Mann, M. (2010). Super-SILAC mix for quantitative proteomics of human tumor tissue. Nat Methods *7*, 383–385. https://doi.org/10.1038/nmeth.1446.

Hengge-Aronis, R., and Fischer, D. (1992). Identification and molecular analysis of glgS, a novel growth-phase-regulated and rpoS-dependent gene involved in glycogen synthesis in Escherichia coli. Molecular Microbiology *6*, 1877–1886. https://doi.org/10.1111/j.1365-2958.1992.tb01360.x.

Houser, J.R., Barnhart, C., Boutz, D.R., Carroll, S.M., Dasgupta, A., Michener, J.K., Needham, B.D., Papoulas, O., Sridhara, V., Sydykova, D.K., et al. (2015). Controlled Measurement and Comparative Analysis of Cellular Components in E. coli Reveals Broad Regulatory Changes in Response to Glucose Starvation. PLOS Computational Biology *11*, e1004400. https://doi.org/10.1371/journal.pcbi.1004400.

Hui, S., Silverman, J.M., Chen, S.S., Erickson, D.W., Basan, M., Wang, J., Hwa, T., and Williamson, J.R. (2015). Quantitative proteomic analysis reveals a simple strategy of global

resource allocation in bacteria. Molecular Systems Biology *11*, 784. https://doi.org/10.15252/msb.20145697.

Irving, S.E., Choudhury, N.R., and Corrigan, R.M. (2021). The stringent response and physiological roles of (pp) pGpp in bacteria. Nature Reviews Microbiology *19*, 256–271. .

Li, G.-W., Burkhardt, D., Gross, C., and Weissman, J.S. (2014). Quantifying Absolute Protein Synthesis Rates Reveals Principles Underlying Allocation of Cellular Resources. Cell *157*, 624–635. https://doi.org/10.1016/j.cell.2014.02.033.

Magnusson, L.U., Nyström, T., and Farewell, A. (2003). Underproduction of ς70 Mimics a Stringent Response: A PROTEOME APPROACH *. Journal of Biological Chemistry *278*, 968–973. https://doi.org/10.1074/jbc.M209881200.

Makman, R.S., and Sutherland, E.W. (1965). Adenosine 3',5'-Phosphate in Escherichia coli. J Biol Chem *240*, 1309–1314. .

Malinverni, J.C., and Silhavy, T.J. (2009). An ABC transport system that maintains lipid asymmetry in the Gram-negative outer membrane. Proceedings of the National Academy of Sciences *106*, 8009–8014. https://doi.org/10.1073/pnas.0903229106.

McBroom, A.J., Johnson, A.P., Vemulapalli, S., and Kuehn, M.J. (2006). Outer membrane vesicle production by Escherichia coli is independent of membrane instability. J Bacteriol *188*, 5385–5392. https://doi.org/10.1128/JB.00498-06.

Moore, R.A., Bates, N.C., and Hancock, R.E. (1986). Interaction of polycationic antibiotics with Pseudomonas aeruginosa lipopolysaccharide and lipid A studied by using dansyl-polymyxin. Antimicrob Agents Chemother *29*, 496–500. .

Neidhardt, F.C. (1996). Escherichia coli and Salmonella: Cellular and Molecular Biology (Washington, D.C: ASM Press).

Notley-McRobb, L., Death, A., and Ferenci, T. (1997). The relationship between external glucose concentration and cAMP levels inside Escherichia coli: implications for models of phosphotransferase-mediated regulation of adenylate cyclase. Microbiology (Reading) *143 (Pt 6)*, 1909–1918. https://doi.org/10.1099/00221287-143-6-1909.

Phaiboun, A., Zhang, Y., Park, B., and Kim, M. (2015). Survival Kinetics of Starving Bacteria Is Biphasic and Density-Dependent. PLOS Computational Biology *11*, e1004198. https://doi.org/10.1371/journal.pcbi.1004198.

Rojas, E.R., Billings, G., Odermatt, P.D., Auer, G.K., Zhu, L., Miguel, A., Chang, F., Weibel, D.B., Theriot, J.A., and Huang, K.C. (2018). The outer membrane is an essential load-bearing element in Gram-negative bacteria. Nature *559*, 617–621. https://doi.org/10.1038/s41586-018-0344-3.

Schaechter, M., MaalØe, O., and Kjeldgaard, N.O. (1958). Dependency on Medium and Temperature of Cell Size and Chemical Composition during Balanced Growth of Salmonella typhimurium. Microbiology, *19*, 592–606. https://doi.org/10.1099/00221287-19-3-592.

Schäfer, U., Beck, K., and Müller, M. (1999). Skp, a molecular chaperone of gram-negative bacteria, is required for the formation of soluble periplasmic intermediates of outer membrane proteins. J Biol Chem *274*, 24567–24574. https://doi.org/10.1074/jbc.274.35.24567.

Schink, S.J., Biselli, E., Ammar, C., and Gerland, U. (2019). Death Rate of E. coli during Starvation Is Set by Maintenance Cost and Biomass Recycling. Cell Systems *9*, 64-73.e3. https://doi.org/10.1016/j.cels.2019.06.003.

Schink, S.J., Polk, M., Athaide, E., Mukherjee, A., Ammar, C., Liu, X., Oh, S., Chang, Y.-F., and Basan, M. (2021). The energy requirements of ion homeostasis determine the lifespan of starving bacteria. 2021.11.22.469587. https://doi.org/10.1101/2021.11.22.469587.

Schmidt, A., Kochanowski, K., Vedelaar, S., Ahrné, E., Volkmer, B., Callipo, L., Knoops, K., Bauer, M., Aebersold, R., and Heinemann, M. (2016). The quantitative and condition-dependent Escherichia coli proteome. Nat Biotechnol *34*, 104–110. https://doi.org/10.1038/nbt.3418.

Schneck, E., Schubert, T., Konovalov, O.V., Quinn, B.E., Gutsmann, T., Brandenburg, K., Oliveira, R.G., Pink, D.A., and Tanaka, M. (2010). Quantitative determination of ion distributions in bacterial lipopolysaccharide membranes by grazing-incidence X-ray fluorescence. PNAS *107*, 9147–9151. https://doi.org/10.1073/pnas.0913737107.

Shi, H., Westfall, C.S., Kao, J., Odermatt, P.D., Anderson, S.E., Cesar, S., Sievert, M., Moore, J., Gonzalez, C.G., Zhang, L., et al. (2021). Starvation induces shrinkage of the bacterial cytoplasm. Proc Natl Acad Sci USA *118*, e2104686118. https://doi.org/10.1073/pnas.2104686118.

Soupene, E., van Heeswijk, W.C., Plumbridge, J., Stewart, V., Bertenthal, D., Lee, H., Prasad, G., Paliy, O., Charernnoppakul, P., and Kustu, S. (2003). Physiological Studies of Escherichia coli Strain MG1655: Growth Defects and Apparent Cross-Regulation of Gene Expression. J Bacteriol *185*, 5611–5626. https://doi.org/10.1128/JB.185.18.5611-5626.2003.

Strange, R.E. (1968). Bacterial “Glycogen” and Survival. Nature *220*, 606–607. https://doi.org/10.1038/220606a0.

Suzuki, H., Nishimura, Y., Yasuda, S., Nishimura, A., Yamada, M., and Hirota, Y. (1978). Murein-lipoprotein of Escherichia coli: a protein involved in the stabilization of bacterial cell envelope. Mol Gen Genet *167*, 1–9. https://doi.org/10.1007/BF00270315.

Tsang, M.-J., Yakhnina, A.A., and Bernhardt, T.G. (2017). NlpD links cell wall remodeling and outer membrane invagination during cytokinesis in Escherichia coli. PLoS Genet *13*, e1006888. https://doi.org/10.1371/journal.pgen.1006888.

Vaara, M. (1992). Agents that increase the permeability of the outer membrane. Microbiol Rev *56*, 395–411. .

Yem, D.W., and Wu, H.C. (1978). Physiological characterization of an Escherichia coli mutant altered in the structure of murein lipoprotein. J Bacteriol *133*, 1419–1426. https://doi.org/10.1128/jb.133.3.1419-1426.1978.

You, C., Okano, H., Hui, S., Zhang, Z., Kim, M., Gunderson, C.W., Wang, Y.-P., Lenz, P., Yan, D., and Hwa, T. (2013). Coordination of bacterial proteome with metabolism by cAMP signalling. Nature *500*, 301–306. https://doi.org/10.1038/nature12446.

Zambrano, M.M., and Kolter, R. (1996). GASPing for Life in Stationary Phase. Cell *86*, 181–184. https://doi.org/10.1016/S0092-8674(00)80089-6.

Supporting Information Figures

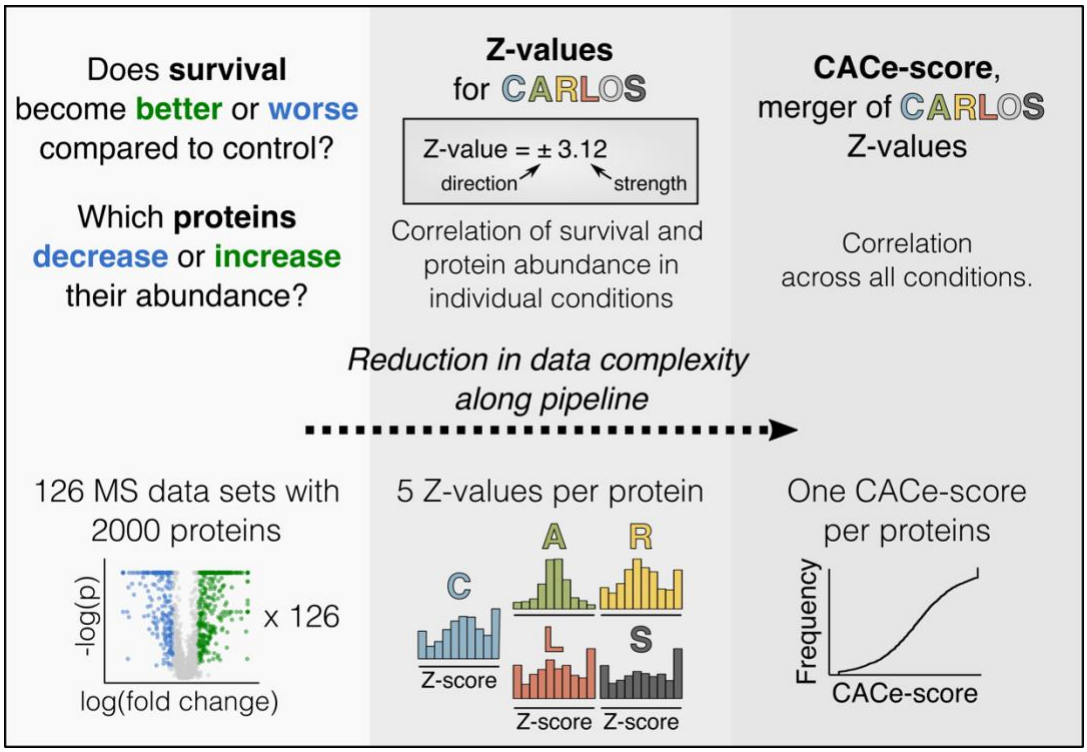

Figure S1 Bioinformatics pipeline. For each CARLOS condition, except 'O' (LacZ overexpression), we evaluate if (1) survival gets better or worse and (2) which proteins significantly increase or decrease their expression, relative to the glucose minimal medium reference condition (left). We exclude 'O', because there were no replicate proteomic measurements available. As in this condition almost all proteins are significantly downregulated (Fig. S2), we expect little new biological information. Each perturbation includes multiple mass spec (MS-) runs corresponding to different perturbation strengths, totaling 126 MS-runs across the CARLOS conditions. The correlation of individual proteins with survival across different MS-runs is merged into a Z-value for each perturbation (center). These five Z-values per proteins are merged into a single 'Combination of Additive Certainties' score (abbr. 'CACe-score') that measures correlation of protein abundance with survival across all experiments (right).

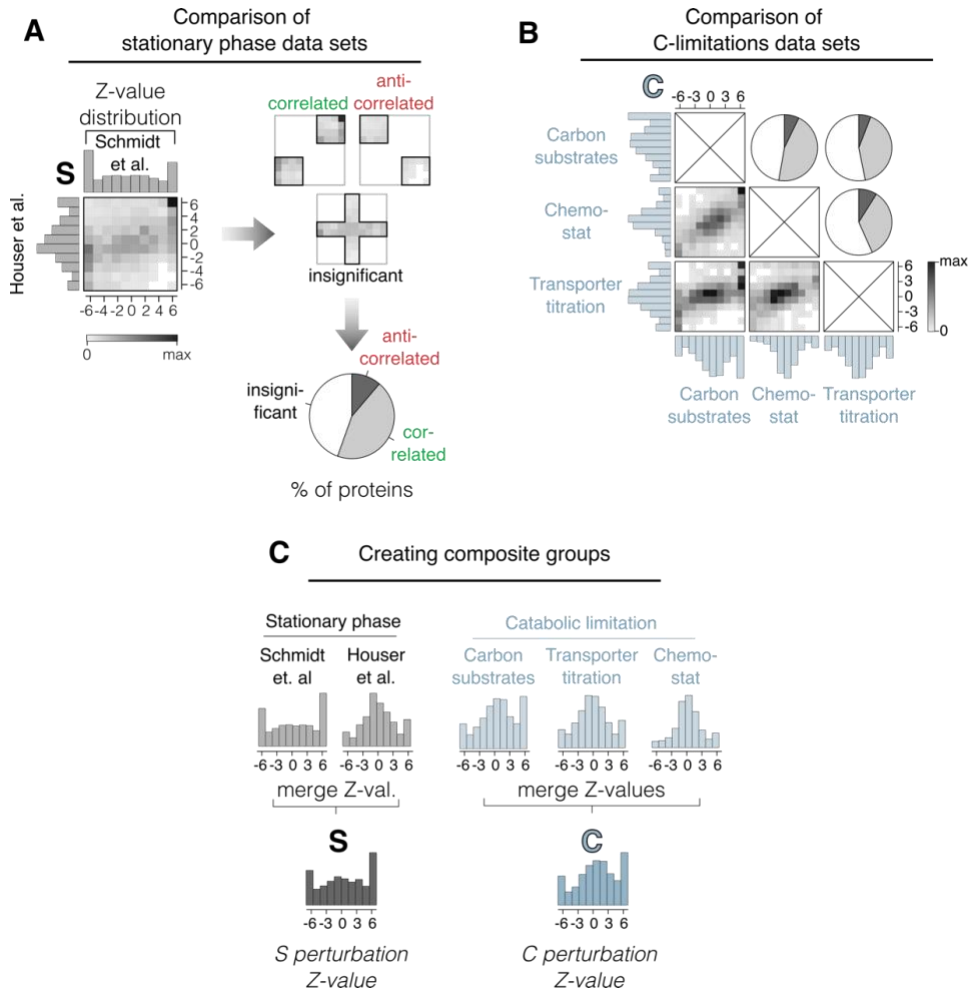

Figure S2 Comparison and merging of MS proteomics data from different sources. (**A**) Comparison of Z-value distributions from two different data sets, by Houser et al. (Houser et al., 2015) and Schmidt et al. (Schmidt et al., 2016), both measured in stationary phase after growth on glucose. On left: Z-value distributions of individual experiments are shown on left and top of correlogram. Shaded area inside the correlogram depicts frequency distribution of individual proteins that are measured in both data sets. On right: Proteins scored in top right and bottom left corner are counted 'correlated', proteins in the top left and bottom right are counted as 'uncorrelated'. Cut-off for significance is chosen at Z = 1.28, corresponding to a p-value of 0.1. Proteins with at least one Z-value less than X are counted as uncorrelated. On bottom: Quantitative analysis of correlation. Only a minority of proteins are observed to anti-correlate between data sets, with the majority either correlating or being statistically insignificant. (**B**) Analysis of correlograms and quantification in pie charts of three data sets of different catabolic limitation analog to panel A. 'Carbon substrates' and 'chemostat' taken from Schmidt et al (Schmidt et al., 2016), 'Transporter titration' taken from Hui et al (Hui et al., 2015). Different types of catabolic limitation show high correlation between data sets. (**C**) Data sets from panel A and B, respectively, are merged to form a single Z-value distribution for each growth perturbation.

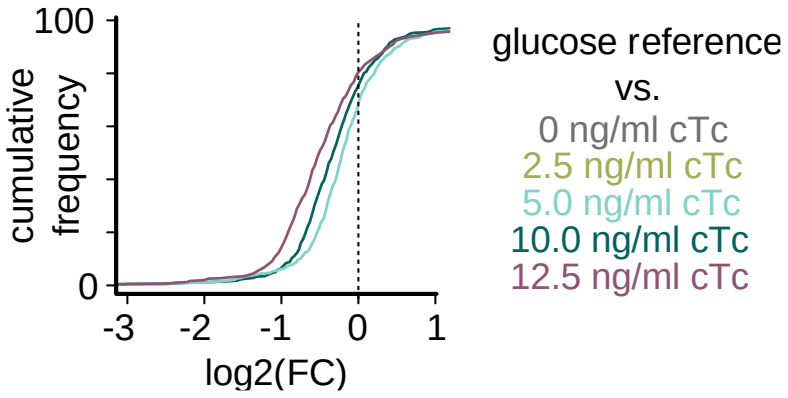

Figure S3 Cumulative distribution of fold-changes. (FC) of protein abundances in LacZ overexpression using strain NQ1389 compared to the reference condition of wild-type E. coli grown on glucose. The abundance of vast majority of proteins decreases with induction of LacZ (inducer: chlortetracycline, cTc).

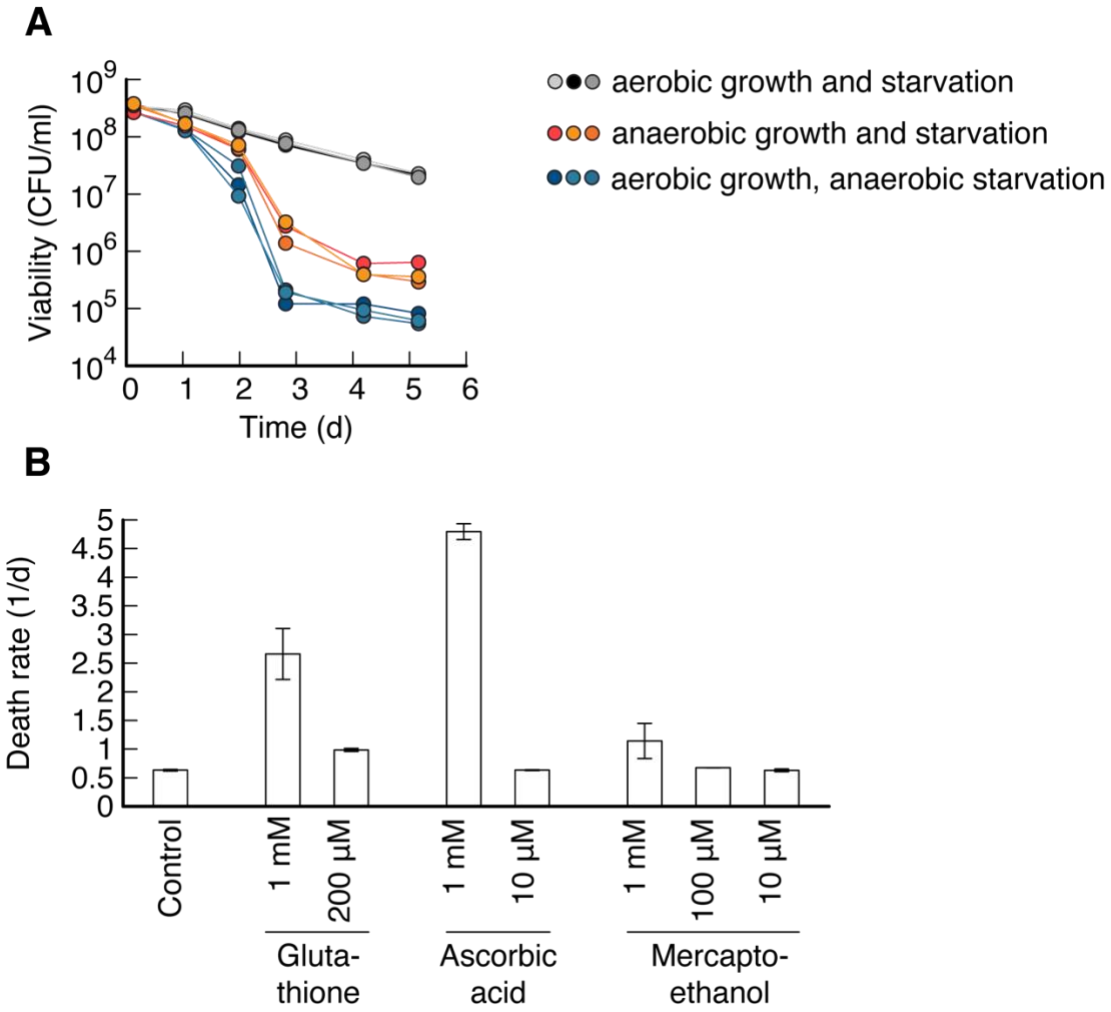

625

626 **Figure S4 Starvation in the absence of oxidative damage.** (**A**) Viability over time in E. coli cultures starved in either
627 anaerobic or aerobic conditions. Cultures previously grown on glucose minimal medium. Neither performing both
628 starvation and growth (orange), nor only starvation in anaerobic conditions (blue) decreased death rate. Instead in
629 both cases, viability decreased several orders of magnitude more compared to aerobic conditions. This finding is in
630 disagreement with previous claims that anaerobic starvation prevents loss of viability (Dukan and Nyström, 1999),
631 but matches the observation that bacteria actively recycle nutrients from dead cells (Schink et al., 2019), which
632 requires oxygen, if bacteria use respiration. (**B**) Starvation in the presence of antioxidants glutathione, ascorbic
633 acid (Vitamin C) and beta-mercaptothanol. High concentrations of antioxidants increase death rate, while low
634 concentrations show no significant effect over control. No antioxidant condition significantly decreased death rate.

635

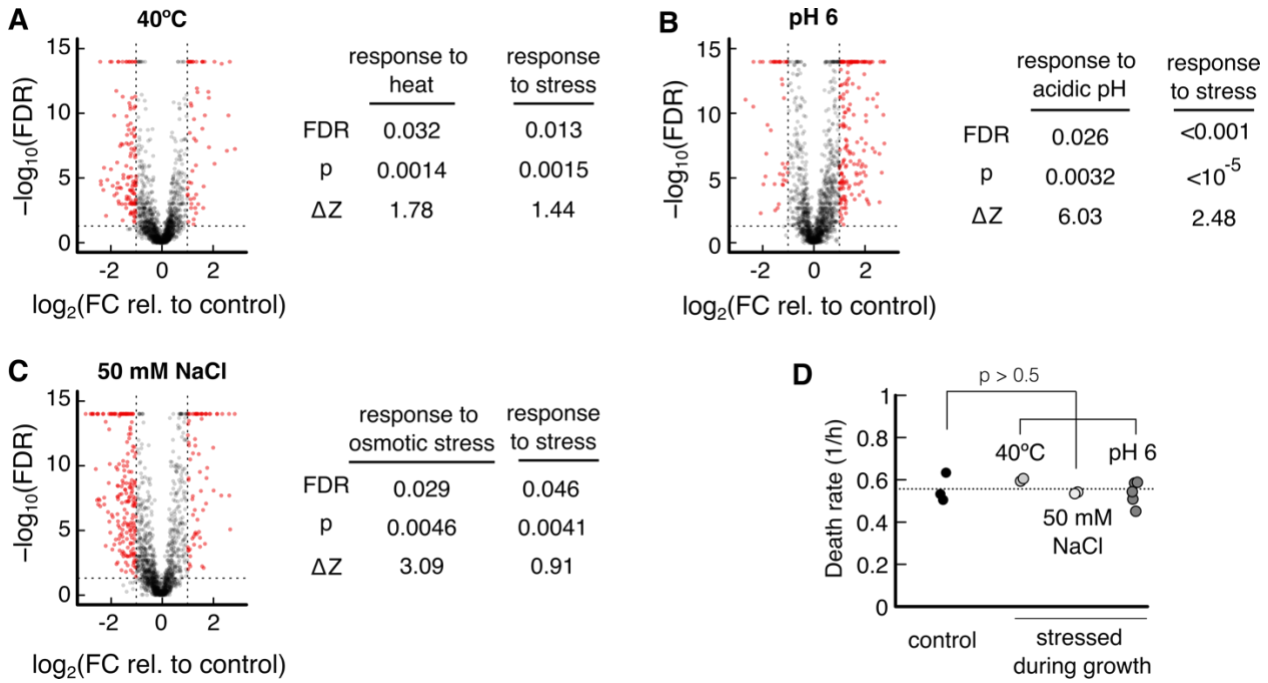

Figure S5 Effect of pre-stressing on proteome and survival kinetics. (**A**-**C**) Comparison of stress conditions to a glucose reference. On left side of each panel, volcano plots of individual proteins, showing the probability of being a response versus the logarithm of the fold change. Proteins with fold change higher than 2 and false discovery rate smaller than 0.05, are colored in red. On the right side of the panel, for each pre-stress (40ºC, pH 6 and 50 mM NaCl), the corresponding stress response and the general 'response to stress' are tested for significant upregulation using Kolmogorov-Smirnov tests. In each pre-stress, both the specific and the general stress response are significantly upregulated, FDR < 0.05. (**D**) After stressing during growth, bacteria are transferred to pre-warmed, carbon-free minimal medium without stress. Death rates of neither pre-stressing condition led to a significant change in death rate.

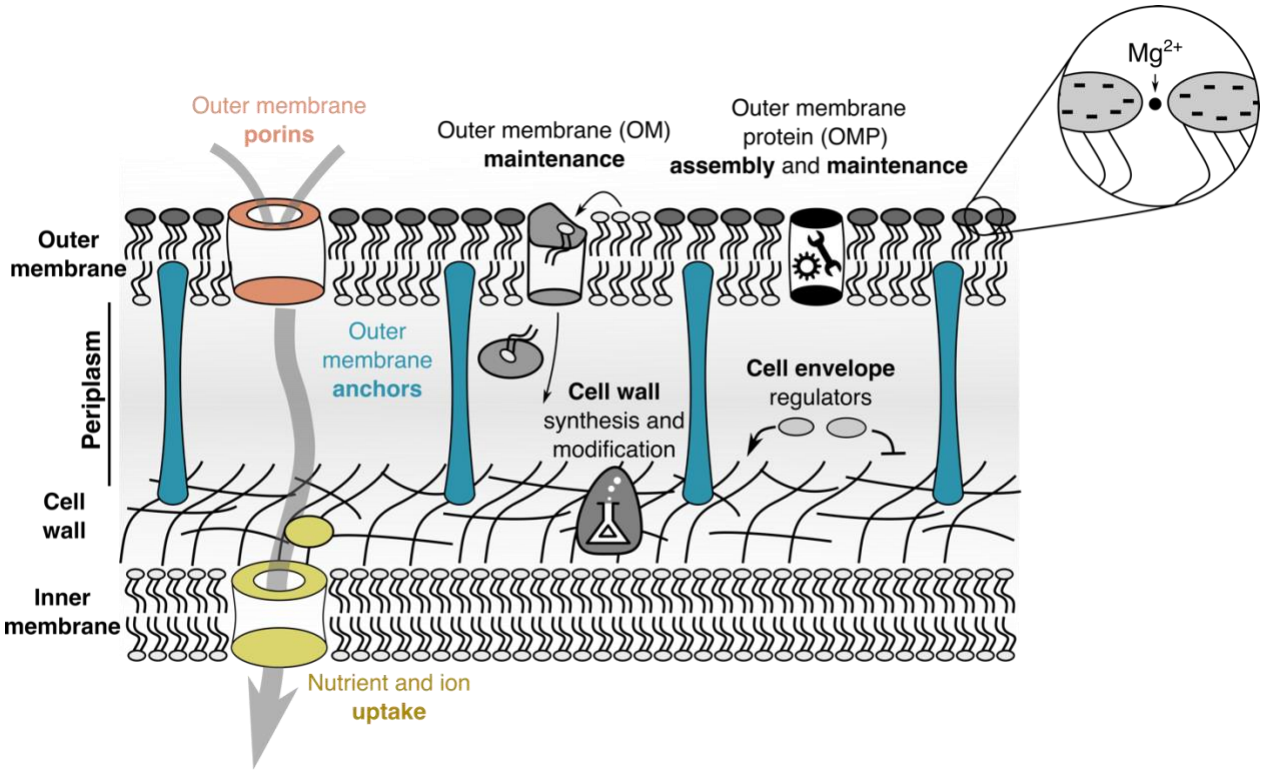

648

649 **Figure S6 The cell envelope of E. coli.** For gram-negative bacteria, the cell envelope consists of the outer
650 membrane, the cell wall, and space between inner and outer membrane called periplasm. Proteins in the cell
651 envelope have diverse functions. Outer membrane anchors (blue), specifically Lpp and OmpA, connect the outer
652 membrane to the cell wall. Outer membrane porins (red) are large tunnel-shaped proteins that facilitate diffusion
653 of biomolecules and ions across the outer membrane. Nutrient uptake systems (yellow) import biomolecules and
654 ions across the inner membrane. While most of the nutrient uptake system is in the inner membrane, thus not
655 considered as part of the envelope, binding proteins (yellow circle in periplasm) are. There are over 100 different
656 kinds of binding proteins in E. coli, which make up a significant fraction of the proteome of the cell envelope. Other
657 proteins include proteins involved in maintenance of the outer membrane, e.g. the mla system which shuffles
658 phospholipids from the outer leaflet of the outer membrane to the inner membrane. Outer membrane protein
659 (OMP) assembly and maintenance are proteins that fold outer membrane proteins, e.g. bam complex, proteases
660 which degrade misfolded proteins, e.g. DegP, and chaperones that prevent folding of outer membrane proteins in
661 solution, e.g. Skp. Cell envelope regulators include the CpxAR signal transduction system and regulation of RpoE via
662 anti-sigma factor RseA. Cell wall synthesis and modification includes cell wall hydrolases and regulators of cell wall
663 synthesis. Lipid A, the lipid on the outer leaflet of the outer membrane is highly charged and requires Mg2+ ions
664 for shielding (Schneck et al., 2010).

665

666 **Supporting Information Tables**

667

668 **Table S1**. Growth and death rates in different growth perturbations. Coloring corresponds to
669 Fig. 1. For all conditions listed here, cultures were washed and resuspended in carbon-free
670 medium. All strains are derived from wild-type *E. coli* K-12 NCM3722. The titratable glutamate
671 synthesis strain NQ393 contains a deletion of gdhA and the promotor of gltBD is replaced by
672 P_{lac}, which is induced with Isopropyl β-D-1-thiogalactopyranoside (IPTG) (Hui et al., 2015). Strain
673 NQ1389 contains two plasmids, P_{tet}-tetR on pZA31 and $P_{tetstab}$-lacZ on pZE1, induced by
674 Chlortetracycline (cTc), allowing high levels of superfluous LacZ expression (Basan et al., 2015a).
675 In addition to Fig. 1A, the table also includes data from a titratable lactose uptake strain NQ381
676 has the P_{lac} replaced by Pu, which is induced with 3-methylbenzyl alcohol (3MBA) (You et al.,
677 2013). This data follows the same trend as other carbon limitations, but is not shown in Fig. 1A.

678

679 **Table S2**. List of Z values, CACe-scores and fold-changes of abundance in pre-stress conditions.
680 A total of 2039 proteins were scored. Values indicated with NA are not available. See Methods
681 for details on the calculation of Z values and CACe-scores. The CARLS columns show the Z
682 values derived as described in the methods. For the C and the S conditions, several datasets
683 were available, which were merged as visualized in Figure S2. The Z values for the individual
684 datasets are also listed as follows: C_chemostat is the chemostat conditions of Ref. (Schmidt et
685 al., 2016), C_carbon_sources is the different carbon growth conditions of Ref. (Schmidt et al.,
686 2016), C_glucose_uptake_titration is the glucose transporter titration set from Ref. (Hui et al.,
687 2015) 'S_houser' is the Z values after 48 h of stationary phase respectively in the study of Ref.
688 (Houser et al., 2015) 'S_schmidt' is the Z values of the stationary phase condition of Ref.
689 (Schmidt et al., 2016). 'HEAT', 'OSM' and 'pH' are Z values of pre-stress conditions with 42ºC,
690 50mM NaCl and pH 6, respectively, of Ref. (Schmidt et al., 2016). 'FC CHvsOSM', 'FC CHvsHEAT'
691 and 'FC CHvsPH' are the fold-changes of protein abundances in pre-stress conditions compared
692 to reference glucose conditions, which are used in Fig. S5.

693

694 **Table S3**. Full list of GO processes and GO compartments and their False discovery rates (FDR)
695 and median CACe-scores.

696 **Table S4**. Absolute abundances of cell envelope proteins, and protein groups in stationary phase,
697 glucose reference condition and LB. See Methods for details on the quantification.

698 **Table S5**. Results from a KO screen. Genes were chosen to have high CACe-scores and to be
699 non-essential. Note that these genes were selected based on a preliminary version of the
700 proteomics analysis, meaning that they do not 100% overlap with the highest scoring set of
701 genes of Table S2. CACe-scores of the final analysis are given in column D. Cultures were grown
702 in N-C- supplemented with NH_4Cl and 20mM glycerol in 96 well plates and starved by letting
703 glycerol deplete. Death rate is estimated from a measurement of viability after glycerol ran out
704 and a measurement after five days of starvation. Each data point is from a single experiment,
705 and the hits were independently verified (Fig. 2). Out of the top five genes, three (*lpp*, *bamE*
706 and *mlaC*) are essential for the cell envelope integrity.
707
708